Gap Junction Dynamics: Reversible Effects of Hydrogen Ions

CAMILLO PERACCHIA and LILLIAN L. PERACCHIA
Department of Physiology, University of Rochester, School of Medicine and Dentistry, Rochester, New York 14642

ABSTRACT Reversible crystallization of intramembrane particle packings is induced in gap junctions isolated from calf lens fibers by exposure to $3 \cdot 10^{-7}$ M or higher $[H^+]$ (pH 6.5 or lower). The changes from disordered to crystalline particle packings induced by low pH are similar to those produced in junctions of intact cells by uncoupling treatments, indicating that H^+, like divalent cations, could be an uncoupling agent. The freeze-fracture appearance of both control and low pH-treated gap junctions is not altered by glutaraldehyde fixation and cryoprotective treatment, as suggested by experiments in which gap junctions of both intact cells and isolated fractions are freeze-fractured after rapid freezing to liquid N_2 temperature according to Heuser et al. (13). In junctions exposed to low pH, the particles most often form orthogonal and rhombic arrays, frequently fused with each other. A number of structural characteristics of these arrays suggest that the particles of lens fiber gap junctions may be shaped as tetrameres.

During the last decade considerable evidence has supported the role of intracellular free calcium ($[Ca^{++}]_i$) or other divalent cations in triggering the membrane mechanisms by which direct cell-to-cell communication via gap junctions is turned off (cell uncoupling) (8, 15, 24). Recently, however, the divalent cation hypothesis has been challenged by data on the independent effect of hydrogen ions in the induction of cell uncoupling (12, 14, 33, 34, 36). The role of H^+, however, has been questioned (32), in view of findings supporting an increase in $[Ca^{++}]_i$, simultaneous with a decrease in pH_i, after various uncoupling treatments. On the other hand, an increase in $[Ca^{++}]_i$ causes a decrease in pH_i (17), hence its uncoupling action could be indirect.

To determine whether divalent cations, hydrogen or both are the uncoupling agents the approach most commonly used (i.e., measurement of coupling resistance between intact cells) is not the ideal one, as in intact cells any uncoupling treatment is expected to simultaneously activate a variety of uncontrollable events which render difficult the unequivocal identification of the uncoupling agents and the directness of their effects on the molecular mechanisms that close the channels. Ideally, one would want to test the independent effect of the postulated uncoupling agents on the permeability of isolated junctions, but the methodologies for measuring gap junction permeability in vitro are not yet available. Meanwhile, the morphological approach (22, 23, 28, 29) provides a reasonable alternative.

In the past, uncoupling treatments have been shown to cause changes in the structure of gap junctions, characterized primarily by a clumping of the intramembrane particles into tight, crystalline arrays, believed to reflect conformational changes with channel occlusion (3, 4, 7, 16, 20, 21, 26, 27). Recently, similar changes have been produced in isolated gap junctions of calf eye lens upon exposure to Ca^{++} or Mg^{++} at neutral pH (1, 22, 23, 25, 29), suggesting that divalent cations affect gap junction structure similarly to in vivo uncoupling treatments. The primary question to which this paper is addressed is whether or not H^+ affects the structure of isolated gap junctions similarly to uncoupling treatments. The data reported here seem to confirm preliminary evidence (28) for the effect of H^+ on the structure of gap junctions at a concentration of $3 \cdot 10^{-7}$ M or higher (pH 6.5 or lower).

MATERIALS AND METHODS

Effects of CO_2 on Rat Lens

The eyes were removed from ether-anesthetized, 1- to 2-mo-old rats (Charles River Breeding Laboratories, Inc., Wilmington, Mass.). The posterior eye walls were sectioned and the lenses carefully dissected out and immediately incubated at 37°C for periods varying from 2 min to 11 h in Tyrode's solutions (29) containing 10–60 mM $NaHCO_3$ (the osmolarity was adjusted to 302 mOsm with NaCl), bubbled with 100% CO_2. The pH of these solutions ranged from 5.7 to 6.6 depending on the bicarbonate concentration. Control lenses were incubated in similar solutions, or in normal Tyrode's solution (29), without CO_2 bubbling. At

THE JOURNAL OF CELL BIOLOGY · VOLUME 87 DECEMBER 1980 719-727

the end of the incubation periods the lenses were fixed by adding 50% glutaraldehyde to the incubation media in the amount necessary to reach the final concentration of 3%. The lenses were kept in this solution at 37°C with CO_2 bubbling for 15–30 min and then fixed for 2–4 h at room temperature in a 3%-glutaraldehyde solution buffered to pH 7.4 with 0.1 M Na cacodylate. The lenses were treated with a 10, 20, 30% series of glycerol solutions in H_2O at 15- to 20-min intervals and freeze-fractured at various depths from the posterior surface with a Balzers BAF 301 freeze-etch unit (Balzers High Vacuum Corp., Santa Ana, Calif.).

Effects of Hydrogen Ions on Isolated Lens Junctions

Pellets of crude gap junction fractions, isolated from calf eye lens as previously described (29), were washed by mild homogenization with a Dounce homogenizer (three strokes) in $1 \cdot 10^{-2}$ M ethylenediaminetetraacetate (EDTA) (Eastman Kodak Corp., Rochester, N. Y.) solutions in which the pH was buffered to values ranging from 6 to 8.5 with $2 \cdot 10^{-2}$ M sodium phosphate. The suspensions were centrifuged for 30 min at 27,000 *g* and the pellets resuspended and incubated in the same solutions for 30 min at 37°C after mild homogenization (20 strokes) with a Dounce homogenizer. At the end of the incubation period the junctions were fixed by mixing the suspensions 1:1 with 6% glutaraldehyde solutions buffered to pH 7.4 with 0.2 M sodium cacodylate. After 15–30 min the suspensions were centrifuged for 30 min at 27,000 *g* and the pellets freeze-fractured with a Denton (Denton Vacuum, Inc., Cherry Hill, N. J.) or a Balzers Freeze-Etch Unit after cryoprotective treatment with 30% glycerol.

Recovery

Experiments aimed at recovering the normal architecture of isolated lens junctions affected by exposure to low pH, were carried out by washing and incubating junctions previously exposed to pH 6 (see above), in $1 \cdot 10^{-2}$ M EDTA or $3 \cdot 10^{-3}$ M (Sigma Chemical Co., St. Louis, Mo.) solutions buffered to pH 7.5 with $2 \cdot 10^{-2}$ M Tris-HCl. In some experiments ATP (#A 3127, Sigma) was added to EDTA or EGTA solutions to a final concentration of $1 \cdot 10^{-3}$ M. Some EGTA-ATP solutions contained $1 \cdot 10^{-4}$ M [Mg^{++}]. At the end of the incubation period (30 min at 37°C) the junctions were fixed in suspension, centrifuged, and freeze-fractured after cryoprotective treatments as previously described.

Rapid Freezing

Unfixed or glutaraldehyde fixed control lenses and pellets of unfixed, isolated lens junctions from controls or pH 6 incubated fractions were rapidly frozen (13) to liquid nitrogen temperature without cryoprotective treatment. Both the intact lenses and the pellets were mounted on Balzers gold specimen carriers glued to the aluminum specimen mount of the rapid freezing machine with dental wax. To prevent excessive flattening of the specimen surface upon impact against the cold copper block of the rapid freezing machine, a brass disk, 7 mm in diameter and 0.4 mm thicker than the specimen carriers, was glued with wax to the center of the aluminum specimen mount. Multiple specimen freezing was performed by mounting four to six specimen holders in a circle around the brass disk. The frozen specimens were stored in liquid nitrogen and fractured within 20 μm from the rapidly frozen surface, using a Balzers freeze-fracture device. To study gap junctions between intact lens fibers, the lenses were frozen from their posterior surface, since there the junctions are more superficial due to the absence of an epithelial layer.

Electron Microscopy

The replicas were examined with an AEI EM 801 electron microscope as previously described (29). Isolated junctions were identified in the electron microscope according to the criteria described in the companion paper (29). In rhombic and orthogonal arrays the particle spacings were measured along the two main axes of the patterns (at 70°–75° and 90° angles, respectively).

RESULTS

Effects of CO_2 on Rat Lens

No structural changes are detected in gap junctions of lens fibers exposed to 100% CO_2 for up to 11 h. In CO_2-treated junctions (Fig. 2) the intramembrane particles and pits are irregularly packed, as in controls (Fig. 1) (5, 23), at a center-to-center distance ranging from 8 to 11 nm. Indeed in ~10% of the experiments crystalline particle packings have been seen in junctions of the most superficial fibers. This phenomenon, however, is not believed to represent a CO_2 effect but rather the consequence of cell injury during dissection, as CO_2 is expected to diffuse quickly throughout the entire depth of the lens and thus should affect deep as well as superficial junctions.

Effects of Hydrogen Ions on Isolated Lens Junctions

93% (Table I) of the lens junctions incubated in Ca^{++} free solutions buffered to pH 6.5 or lower assumed crystalline particle packing (Fig. 4), while all the junctions exposed to similar solutions buffered to pH 6.6 or higher maintained irregularly packed particle arrays (Fig. 3) typical of controls. Curiously, the crystalline arrays are most often orthogonal or rhombic (Figs. 4, 5, and 7 *d* and *e*; references 8–10). Junctions with irregularly packed particles are often curved (Figs. 3 and 6) while junctions with crystalline arrays are distinctively flat (Figs. 4 and 5). In crystalline arrays the center-to-center distance between neighboring particles or pits is 6.5–7 nm, while in loosely packed arrays it is similar to that of intact fiber junctions (8–11 nm).

Recovery

Over 80% (Table II) of the junctions induced to crystallize (Fig. 5) by exposure to Ca^{++}- and Mg^{++}-free solutions buffered to pH 6 recover a control appearance (loosely packed particle arrays) (Fig. 6), upon incubation in similar solutions buffered to pH 7.5. Addition of $1 \cdot 10^{-3}$ M ATP with or without $MgCl_2$ (to a final [Mg^{++}] of $1 \cdot 10^{-4}$ M) to the recovery solutions does not improve the frequency of recovery.

Rapid Freezing

In freeze-fracture, gap junctions between superficial cells of the posterior lens wall, rapidly frozen (13) to liquid nitrogen temperature without fixation and cryoprotective treatment (Fig. 7 and 7 *a*), do not differ from junctions prepared by conventional methods (Fig. 1). Glutaraldehyde fixation before rapid freezing does not modify the junctional appearance (Fig. 7 *b*). The rapid freezing method was also applied to unfixed, uncryoprotected pellets of isolated lens fiber junctions incubated in Ca^{++}- and Mg^{++}-free solutions buffered to pH 7 (Fig. 7 *c*) or pH 6 (Fig. 7 *d* and *e*). In both cases the junctions do not differ from fixed and cryoprotected junctions freeze-fractured by the conventional method after similar incubation treatments (Figs. 3 and 4, respectively).

In rapidly frozen specimens the intramembrane particles of both gap junctions and perijunctional regions always appear well defined. This was also noticeable in isolated uncryoprotected junctions conventionally freeze-fractured and deeply etched (29). In other preparations, however, the particles are often ill-defined, varying in size and shape and apparently fusing with each other to form rod or fibril-like images. Since in both the rapid freezing and deep etching procedures glycerol treatment is avoided, this phenomenon could be an artifact caused by such treatment.

Crystalline Patterns

In junctions freeze-fractured after incubation at pH 6, the particles aggregate into two distinct types of crystalline patterns: orthogonal (Figs. 4, 5, 8, and 9) and rhombic (Figs. 5, 8,

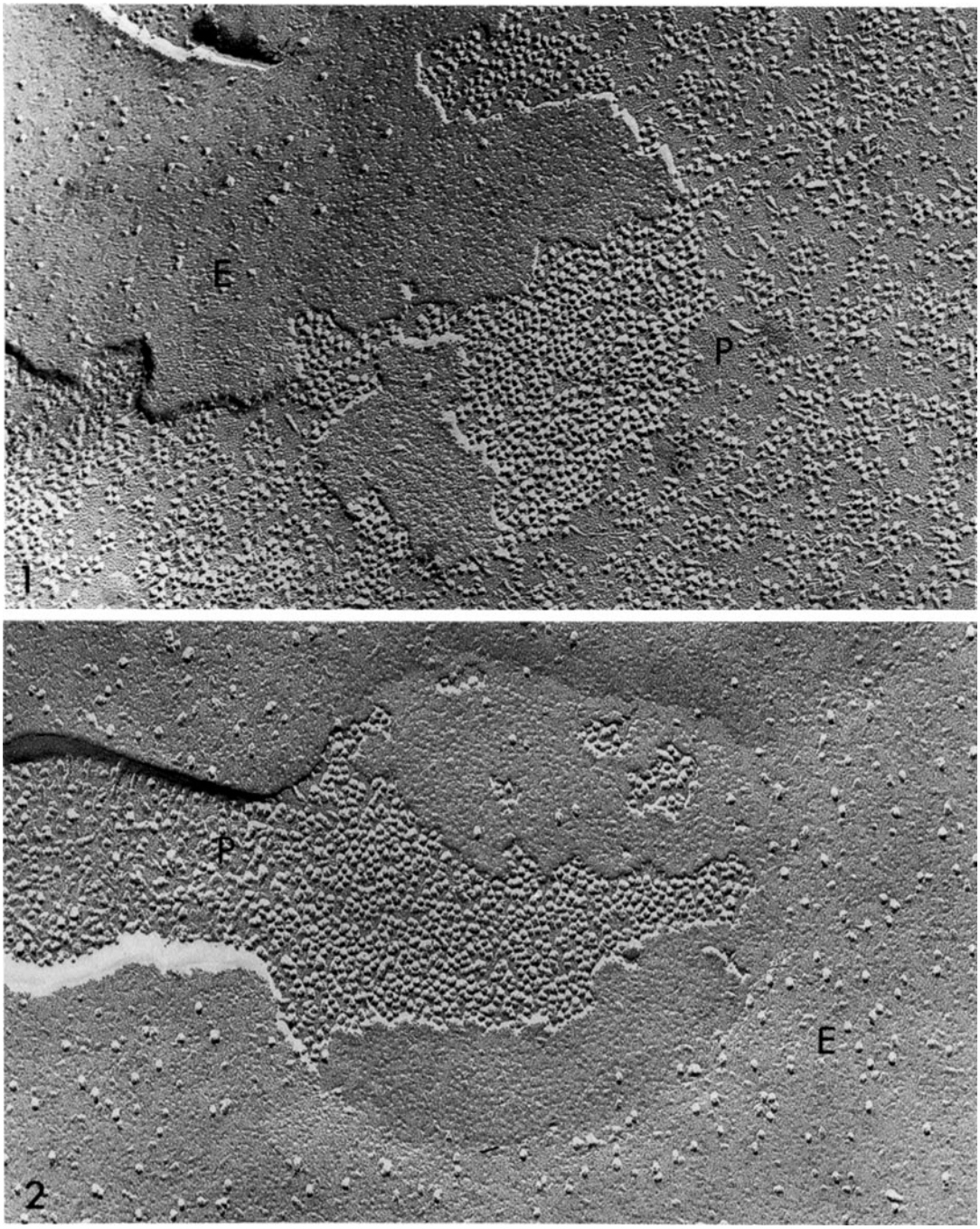

FIGURE 1 Freeze-fracture replica of a gap junction between rat lens fibers (control). The fracture plane steps down from E face (*E*) to P face (*P*). Gap junction particles and pits are irregularly packed at a center-to-center distance ranging from 8 to 11 nm. × 123,600.

FIGURE 2 Freeze-fracture replica of a gap junction between rat lens fibers incubated for 15 min at 37° in a Tyrode's solution containing 20 mM $NaHCO_3$ and vigorously bubbled with 100% CO_2. Notice that particles and pits are disorderly packed as in control junctions (Fig. 1). *P*, P face; *E*, E face. × 123,600.

and 10). "Rhombic" is used here in reference to arrays built on rhombic unit cells with acute angles of 70°–75°. Typical hexagonal arrays, often seen after Ca^{++} and/or Mg^{++} exposure (29) are rare at low pH. Interestingly, orthogonal and rhombic patterns are often fused with each other (Fig. 8) in such a way that the orientation of only one of the two axes, on which pits or particle rows are aligned, changes. This feature is shown in Fig. 8 (areas *A* and *B*). In Fig. 8 (area *A*) the vertical rows of pits remain parallel to each other and maintain roughly the same periodicity in both the orthogonal (left) and the rhombic (right) pattern, while the horizontal rows bend upward sharply where the two patterns meet such that the angle between the axes of the pattern changes from ~86° (left) to ~71° (right). Similarly, in Fig. 8 (area *B*) only the vertical rows change orientation, so that the angle between the axes of the pattern changes from ~90° (bottom) to ~70° (top). Fusions between rhombic patterns are also seen. In Fig. 10 the horizontal rows remain parallel to each other along the whole junction, while

TABLE I

Hydrogen Effects on the Crystallinity of Particle Packing in Isolated Lens Fiber Gap Functions

$[H^+]$	Percent of crystalline junctions	No. of junctions studied	No. of experiments performed
$3 \cdot 10^{-7}$ M or higher (pH 6.5 or lower)	93	105	13
$2.5 \cdot 10^{-7}$ M or lower (pH 6.6 or higher)	0	165	16

TABLE II

Recovery from H^+ Effect on the Crystallinity of Particle Packing in Isolated Lens Fiber Junctions

	Percent of crystalline junctions	No. of junctions studied	No. of experiments performed
$1 \cdot 10^{-6}$ M $[H^+]$ (pH 6)	95.6	91	6
$3 \cdot 10^{-8}$ M $[H^+]$ (pH 7.5), after exposure to pH 6 as above	17.6	85	12

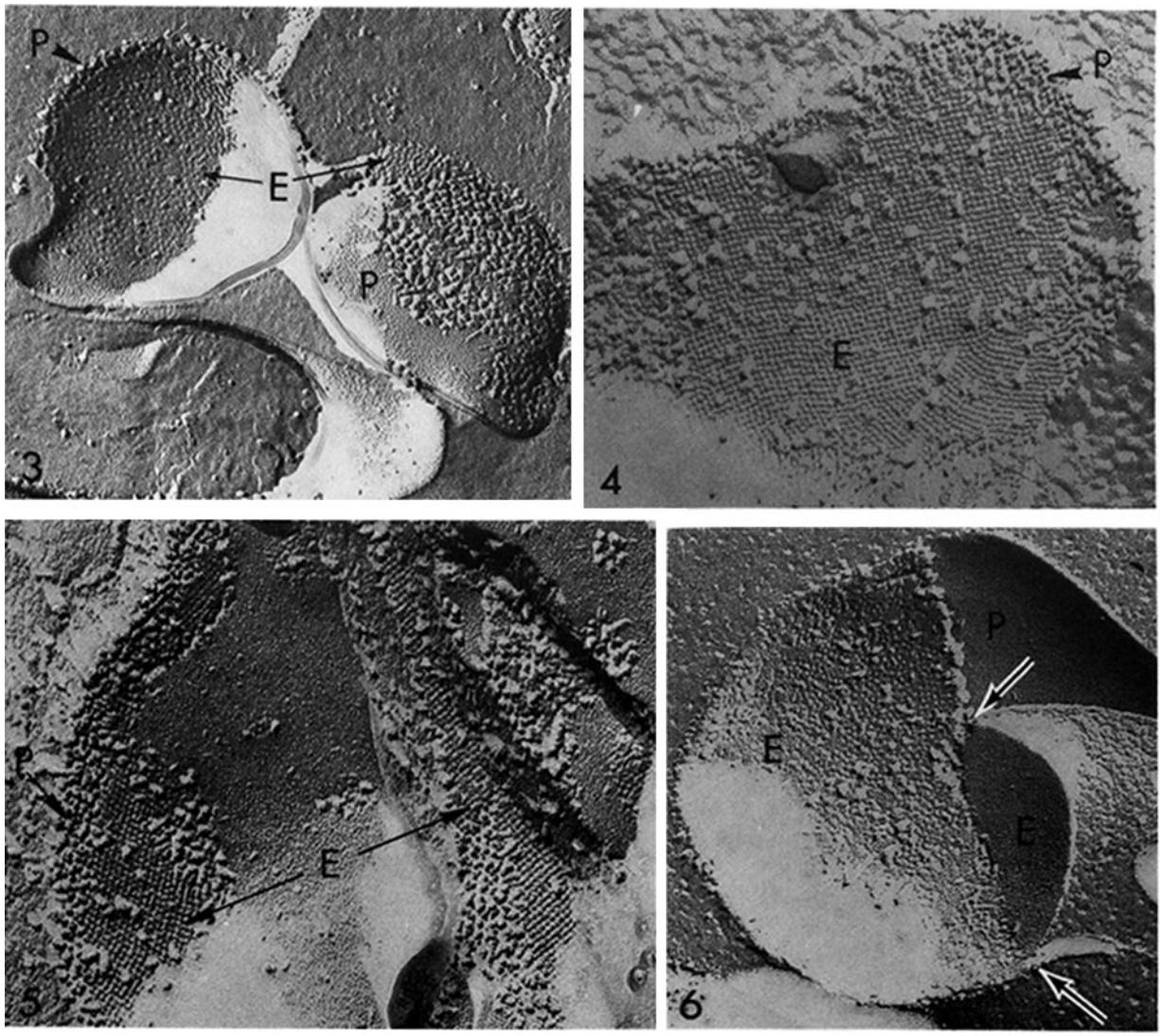

FIGURE 3 Freeze-fracture replica of a gap junction isolated from calf lens fibers, in the presence of EDTA, and subsequently incubated in a Ca^{++}-, Mg^{++}-free solution buffered to pH 6.7. Notice that the junctional pits are irregularly packed as in control junctions. *P*, P face; *E*, E face. × 123,600.

FIGURE 4 Freeze-fracture replica of a gap junction isolated from calf lens fibers, in the presence of EDTA, and subsequently incubated in a Ca^{++}-, Mg^{++}-free solution buffered to pH 6.4. Notice that particles and pits are packed into a crystalline array (mostly orthogonal), at a center-to-center spacing of 6.5–7 nm. *P*, P face; *E*, E face. × 123,600.

FIGURE 5 Freeze-fracture replica of a gap junction isolated from calf lens fibers, in the presence of EDTA, and subsequently incubated in a Ca^{++}-, Mg^{++}-free solution buffered to pH 6. Notice that particles and pits are packed regularly into orthogonal and rhombic arrays. *P*, P face; *E*, E face. × 123,600.

FIGURE 6 Freeze-fracture replica of a gap junction isolated from calf lens fibers, in the presence of EDTA, incubated in a Ca^{++}-, Mg^{++}-free solution buffered to pH 6 and subsequently incubated in a Ca^{++}-, Mg^{++}-free solution buffered to pH 7.5 (recovery solution). Notice that the pits are irregularly packed at a center-to-center distance ranging from 8 to 11 nm as in controls (Fig. 3). *E*, E face; *P*, P face. × 123,600.

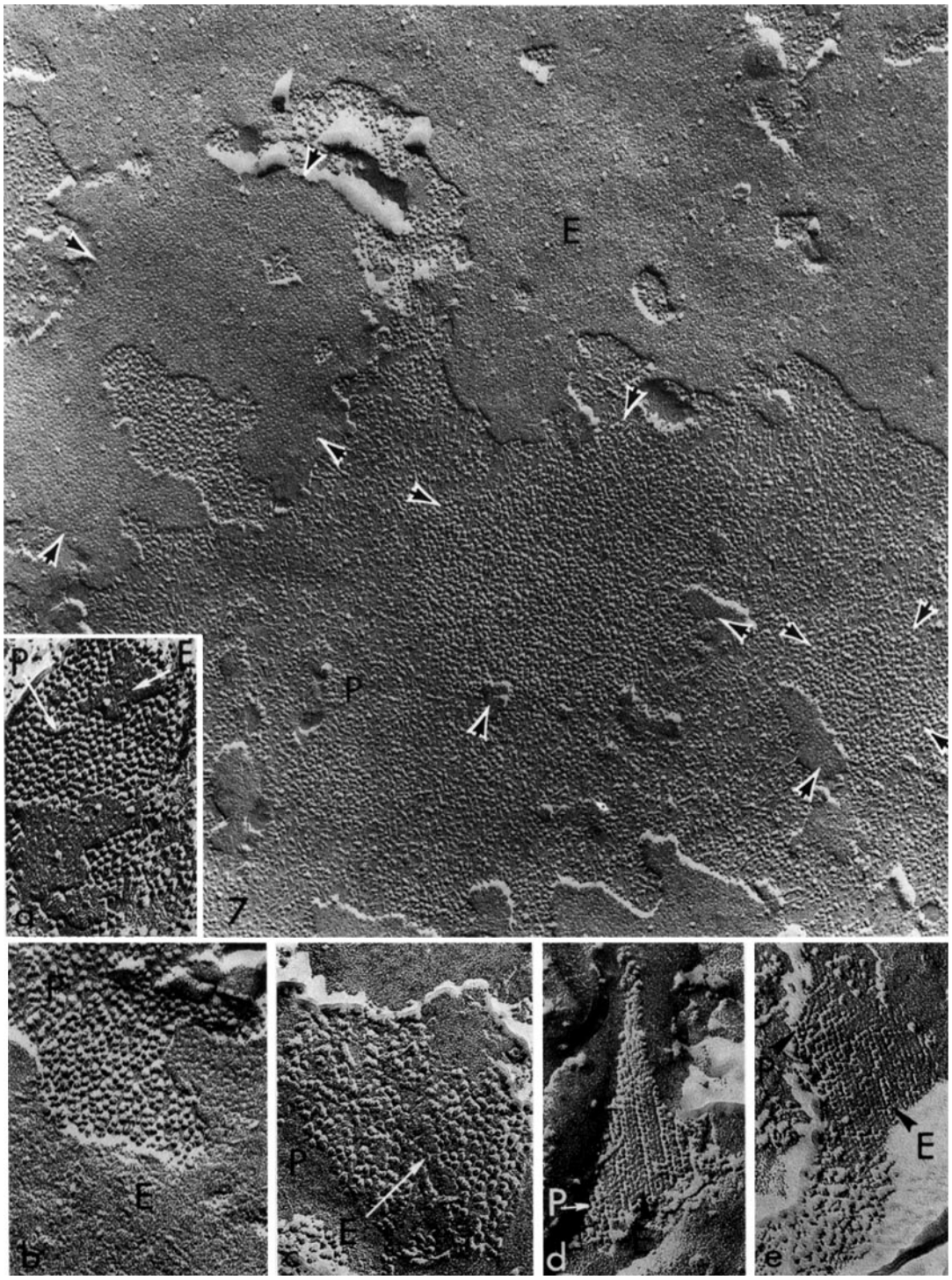

FIGURE 7 Freeze-fracture replica of a gap junction from intact, untreated rat lens fibers rapidly frozen (13) to liquid N_2 temperature without glutaraldehyde fixation and cryoprotective treatment. Three junctions (arrows) are recognizable as patches of aggregated particles or pits. Notice that particles and pits are disorderly packed at a center-to-center distance similar to that of glutaraldehyde fixed and glycerol treated gap junctions, freeze-fractured by conventional methods (Fig. 1). *Inset* (*a*) shows, at higher magnification, a similar rat lens fiber gap junction rapidly frozen without glutaraldehyde fixation and glycerol treatment. *b* Shows a rat lens fiber gap junction rapidly frozen after glutaraldehyde fixation (uncryoprotected). *c* Shows a gap junction isolated from calf lens, in the presence of EDTA, incubated in a Ca^{++}-, Mg^{++}-free solution buffered to pH 7 and rapidly frozen without glutaraldehyde fixation and glycerol treatment. *d* and *e* Show gap junctions isolated from calf lens fibers, incubated in a Ca^{++}-, Mg^{++}-free solution buffered to pH 6 and rapidly frozen without glutaraldehyde fixation and glycerol treatment. Notice that particles and pits maintain, after rapid freezing, either disordered (*a* and *c*) or crystalline (*d* and *e*) packings similar to those of glutaraldehyde fixed, conventionally freeze-fractured junctions exposed to the same treatment (Figs. 1, 3, and Figs. 4, 5, and 8–10, respectively). P = P face; E = E face. × 77,000. *Insets*, × 123,600.

the vertical rows bend sharply to the right, approximately at the center of the pattern, such that the two axes form a 70°–75° angle open to the lower right in the bottom pattern and a similar angle open to the upper right in the top pattern. In Fig. 8 (area *C*) a fault in the pattern, possibly caused by a foreign particle (white arrow) trapped in the junction during the crystallization process, induces the horizontal rows to change direction sharply, below the white arrow, before regaining their original orientation; in both regions the pits form rhombic arrays as the angle between the two axes is ~71° in one pattern and ~73° in the other. Here also, one of the two axes (the vertical one) does not change orientation. This feature is clearly seen by tilting the micrograph sharply and observing each of the patterns of Figs. 8 and 10 along the direction of the unbent rows. Interestingly, by observing the patterns on tilted micrographs one would not suspect the presence of two types of crystalline packings. Although in some cases rhombic arrays could be distorted hexagonal arrays or products of tilted replica surfaces, the limited range of angle values in these arrays, their high frequency in low pH preparations, and their precise relationship with orthogonal arrays suggest that they are in fact real structures.

A tentative interpretation of the molecular basis of the orthogonal and rhombic patterns is shown in Figs. 11–13. Here the intramembrane particles are schematically depicted as tetrameres. Orthogonal patterns, due to a side-by-side aggregation of the tetrameres, would change into rhombic ones (with angles of 70°–75°) as a result of a sliding of tetramere rows, along one of the two axes, for lengths equal to one-fourth the tetramere side length (Fig. 11). Pattern features such as those shown in Figs. 8 (area *C*) and 10 could also be explained by this model (Figs. 12 and 13, respectively). Interestingly, tetrameres could also form slightly distorted hexagonal arrays (Fig. 14).

DISCUSSION

The data reported in this study indicate that gap junctions isolated from mammalian lens fibers undergo structural changes when subjected media free of Ca^{++} and Mg^{++} and buffered to pH 6.5 or lower. Such changes, characterized by the formation of crystalline particle packings, are similar to changes seen in junctions of intact cells subjected to uncoupling treatments (3, 4, 7, 16, 20, 21, 26, 27), and in isolated lens junctions exposed to uncoupling agents such as Ca^{++} or Mg^{++} (22–25, 29). Thus H^+ could also be an uncoupling agent (33, 34).

Curiously, exposure of intact lenses to 100% CO_2 does not change the particle packing of fiber junctions. It could be that the junctions are less sensitive to low pH in intact cells, but most likely the high protein content of the fiber cell cytoplasm provides them with an unusually high buffering capacity for H^+. Indeed, in other cell systems crystalline particle packings have been seen in gap junctions upon exposure to 100% CO_2 (16), indicating that also in intact cells gap junctions crystallize when $[H^+]_i$ increases above normal values.

Recently, some questions have been raised on the capacity of lens fiber junctions to assume crystallinity as well as to change their permeability properties, such that the junctions have been called noncrystallizing, nonregulated low resistance junctions (10). From the ultrastructural point of view we feel that our quantitative data on the effects of divalent cations and H^+ reported in this and previous papers (23, 28, 29), and recently confirmed by others (1), provide convincing evidence for the ability of isolated junctions to crystallize. Moreover, recent data on the widespread crystallization of gap junctions between rat lens fibers (25) treated by methods that increase the intracellular calcium-content (9) clearly indicate that fiber gap junctions are also capable of crystallization in the intact lens.

Attempts to electrically uncouple lens fiber junctions have been thus far unsuccessful; however, this is not surprising as one would expect lens fibers to be particularly resistant to uncoupling treatments. In fact, their mainly glycolytic metabolism renders inoperative most uncoupling methods such as treatments with DNP, cyanide, asphyxia, etc. The virtual absence of mitochondria and reticulum in these cells impairs methods which rely on Ca^{++} release from internal stores. The high protein content of these cells suggests a high Ca^{++} and H^+ buffering capacity. The location of lens fibers, far removed from the surface of the organ, and the extremely narrow and convoluted extracellular space, protect the cells from mechanical injury and drastic changes in the extracellular medium, and finally, the unusual shape of these cells (they are narrow tubes a few micrometers wide and several millimeters long) discourages uncoupling attempts by intracellular Ca^{++} injection, as it seems unlikely that the $[Ca^{++}]_i$ would change in cellular regions far away from the injecting micropipettes. On the other hand, evidence for the ability of lens fibers to "heal

FIGURE 8 Freeze-fracture replica of gap junctions isolated from calf lens fibers and incubated at pH 6. Several patches of crystallinity are shown. Particles and pits are arranged into orthogonal and rhombic arrays. Areas *A* and *B* show that the two types of packing are continuous with each other, and that the change from one to the other follows a shift in the orientation of only one of the two axes on which particle rows are aligned. In area *A*, the vertical rows of pits remain parallel to each other in both the orthogonal (left) and the rhombic (right) pattern, whereas the horizontal rows bend sharply upward, where the patterns meet, changing the angle from 86° to 71° (see Fig. 11). Similar behavior is shown in area *B*, as indicated by the three arrows. In area *C*, the horizontal axis of the rhombic pattern bends downward for a short length and then regains its original orientation (as shown by the three arrows drawn below the pattern). The angle between the axes is 70°–75° in both but the arrays are mirror symmetrical. The shift in the pattern may result from a downward sliding of two vertical rows of particles (pits) (see Fig. 12), caused by a foreign particle (white arrow) trapped in the junction during the crystallization process. The black and white arrows point to the regions where two membranes meet to form a gap junction. *P*, P face; *E*, E face. × 144,000.

FIGURE 9 Freeze-fracture replica of a gap junction isolated from calf lens fibers, in the presence of EDTA, and incubated at pH 6. Particles and pits are packed into two orthogonal arrays joined together at an angle. *P*, P face; *E*, E face. × 123,600.

FIGURE 10 Freeze-fracture replica of a gap junction isolated from calf lens fibers, in the presence of EDTA, and incubated at pH 6. Particles and pits are packed into rhombic arrays. The horizontal rows remain parallel to each other along the whole junction, whereas the vertical rows bend sharply to the right approximately at the center of the junction. The two arrays have similar angles between their main axes (70°–75°) but they are mirror symmetrical (see Fig. 13). *P*, P face; *E*, E face. × 123,600.

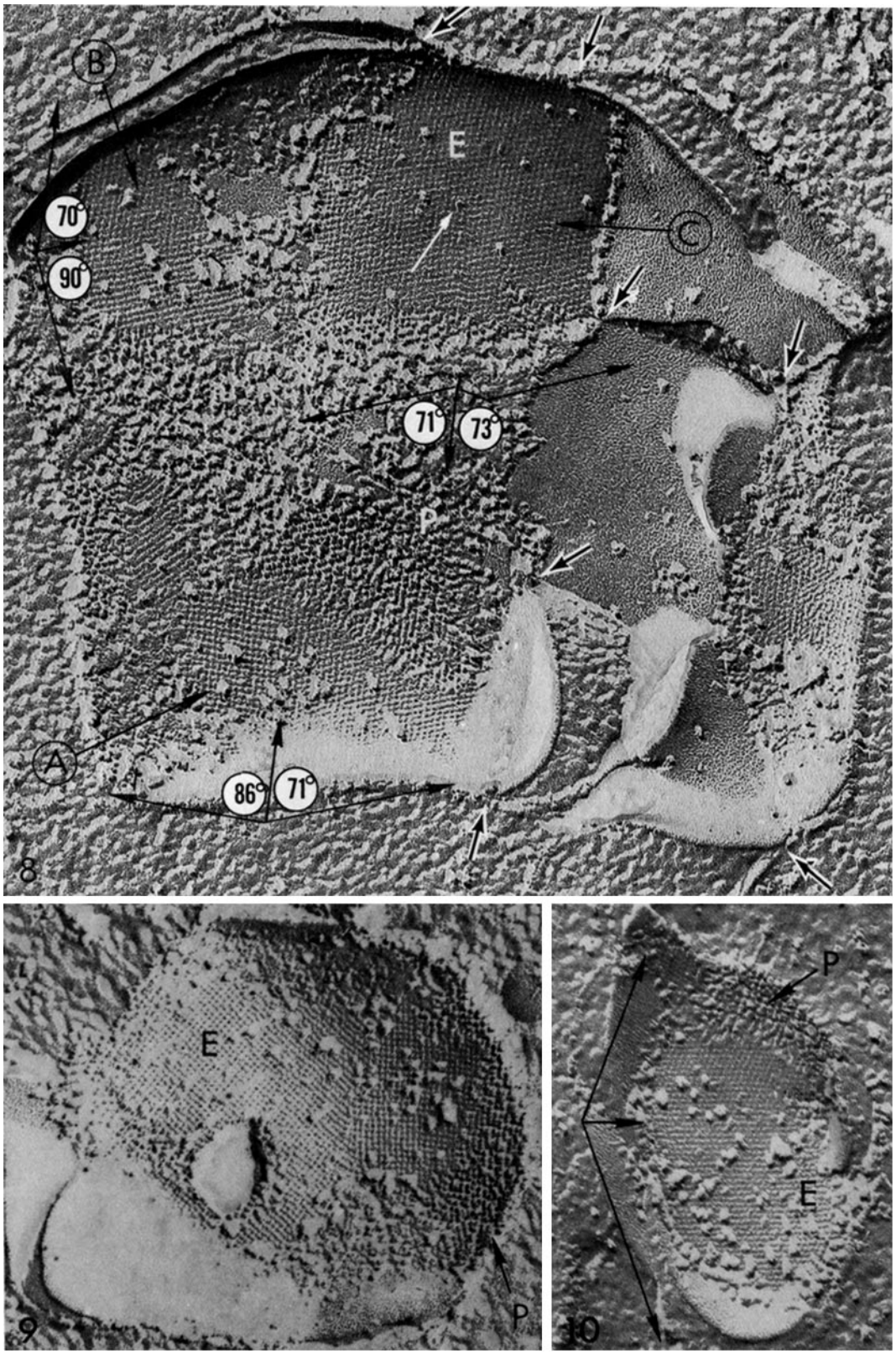
B
E
70°
90°
C
71°
73°
P
A
86°
71°
8
E
P
9
P
E
10

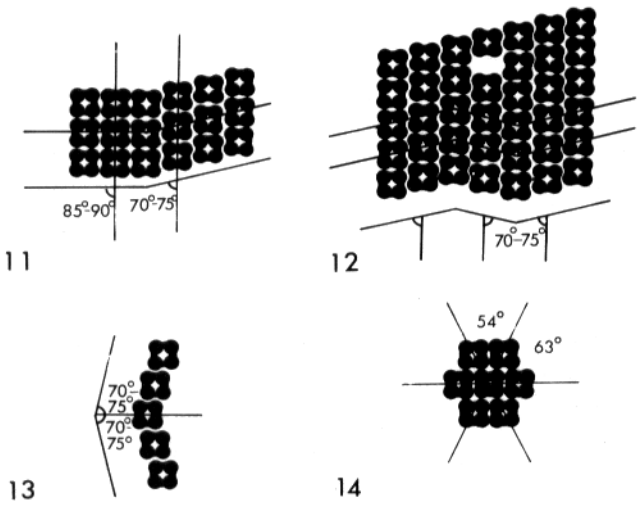

FIGURES 11–14 Diagrammatic interpretation of the molecular architecture of crystalline arrays in lens fiber junctions. The presence of both orthogonal and rhombic arrays can be best explained by assuming that the particles are shaped as tetrameres. Orthogonal patterns, produced by a side by side aggregation of the tetrameres, would become rhombic (with a 70°–75° angle) as a result of a sliding of tetramere rows, along one axis, for distances equal to one-fourth of the tetramere side length, such that the tetrameres are interlocked along one axis and are packed side by side along the other. Interestingly, a sliding of the rows along one axis for a distance equal to one-half the tetramere side length (Fig. 14), would cause tetrameres to pack in nearly hexagonal arrays. Figs. 11, 12, and 13 depict regions similar to those shown in Figs. 8 (areas *A* & *B* and *C*), and 10, respectively.

over" (2, 6, 31) indicates that also these cells are capable of uncoupling. Interestingly, in the lens, as in the heart (8), the healing-over process, determined by measuring the time course of the ^{42}K-fractional loss after mechanical injury, depends on the presence of external Ca^{++} (6).

The lowest $[H^+]$ to affect gap junction structure is close to that reported to trigger uncoupling in *Xenopus* embryo (33, 34); however, it might be different in intact lens fibers as a result of possible competition between H^+ and other ions to the junctional sites (24, 25). Similarly to divalent cations (29), recovery from the pH effects does not require ATP, once more suggesting that the structural changes may follow a simple binding and unbinding of the uncoupling agent to the junctional proteins. Applying to the H^+ effect the hypothesis proposed for the effect of divalent cations (24, 25, 29), one could envision hydrogen ions triggering conformational changes by neutralizing negative charges on the protein.

Alternatively, H^+ could enhance the affinity of the junctional molecules toward Ca^{++} and/or other divalent cations. In our experiments on isolated junctions the various solutions used to test the H^+ effects contained $1 \cdot 10^{-2}$ M EDTA, which, at pH 7, would bring the $[Ca^{++}]$ to $1 \cdot 10^{-10}$ M, for an assumed Ca^{++} contaminant concentration of $1 \cdot 10^{-5}$ M. Indeed, with a decrease in pH the final $[Ca^{++}]$ is expected to rise as a result of an increase in the EDTA-Ca K_D, but even at pH 6 the $[Ca^{++}]$ would remain below $1 \cdot 10^{-8}$ M, and thus much lower than that ($5 \cdot 10^{-7}$ M) reported to affect gap junction structure at pH 7 (23, 24, 29). Such $[Ca^{++}]$, however, could be effective on the junctions at pH 6.5 or lower. Interestingly, the uncoupling effect of acetylcholine (ACh) on pancreatic cells is enhanced when pH_i is decreased with 20% CO_2 and is reduced when pH_i is increased with 10 mM NH_4Cl (14). Although these data could be interpreted in a number of ways, the possibility that changes in pH_i modulate the sensitivity of the junctional molecules to similar changes in $[Ca^{++}]$, brought about by ACh treatment, should be kept in mind.

The rapid freezing experiments indicate that the pattern of particle aggregation is not affected by glutaraldehyde; thus, our data confirm similar observations on mammalian heart (4). In fact, if glutaraldehyde were causing crystallization by directly affecting the junctional molecules (30), one would expect virtually all junctions yet studied to be crystalline, as they are all glutaraldehyde fixed. That this is not the case has been demonstrated quantitatively, aside from the present study, in a variety of vertebrate and invertebrate cells (i.e., references 3, 4, 7, 11, 21, 23, 27, 29). In certain cells, however, glutaraldehyde could cause a sudden increase in Ca^{++} influx, with junction crystallization, possibly as a consequence of membrane depolarization.

Differently from other vertebrate gap junctions, lens fiber junctions exposed to low pH form, most often, orthogonal or rhombic particle packings. Although hexagonal packings seen in other junctions are often slightly distorted such that the particle rows meet only rarely at precise 60° angles, the rhombic arrays of lens junctions are not likely to be distorted hexagonal packings in view of their well-defined relationship with orthogonal arrays and the limited range of angle values (70°–75°). As shown in the diagrams (Figs. 11–13), the architecture of the two arrays can be best explained by assuming that the particles of lens fiber junctions are shaped as tetrameres. There is evidence that the particles of other gap junctions may be shaped as hexameres (11, 18, 19, 24, 35). Hexameres, however, would not aggregate regularly into orthogonal arrays. On the other hand, tetrameres could also be arranged into nearly hexagonal patterns (Fig. 14).

Another peculiarity of lens junctions is the unusual tightness of the crystalline packings, as in either the hexagonal (29), the rhombic, or the orthogonal arrays, the center-to-center distance between neighboring particles is shorter than that of other crystalline junctions of vertebrates (24) by 1.5–2 nm. In addition, preliminary measurements (Peracchia, unpublished observations) indicate that the overall thickness of isolated lens junctions is smaller than that of isolated liver junctions by ~2 nm, possibly because of a narrower extracellular gap, a structural feature which may account for the low permeability of the gap to extracellular tracers and negative stains (5, 10). These morphological peculiarities could all be the consequence of differences in protein structure between these and other vertebrate gap junctions, possibly resulting in smaller particles.

Interestingly, the intramembrane particles appear as more distinct and better defined units in freeze-fracture replicas of tissues rapidly frozen or deeply etched after conventional freeze-fractures (29). Since in both preparations glycerol treatment is avoided, we are inclined to believe that particle deformation and apparent particle fusion, often seen in conventional specimens, are caused by glycerol. It seems possible in fact that glycerol weakens the interaction between ice and the hydrophilic ends of the particles, such that during fracture some of the particles may be partially pulled out of the membrane leaflet and slightly misplaced. This is also supported by the usual observation of a more precise crystallinity in pitted than in particulated fracture faces.

In conclusion, this and the preceding paper (29) indicate that structural changes reported in gap junctions of intact cells with functional uncoupling are likely to be a direct effect of uncou-

pling agents such as Ca^{++}, Mg^{++}, and H^{+} on the junctional molecules. The changes in particle packing and channel permeability are believed to follow neutralization of negative charges on Ca^{++} sites at the junctional proteins.

This research was supported by a grant from the National Institutes of Health (GM 20113).

Received for publication 27 February 1980, and in revised form 17 July 1980.

REFERENCES

1. Alcala, J., J. Kuszak, M. Katar, R. H. Bradley, and H. Maisel. 1979. Relationship of intrinsic and peripheral proteins to chicken lens gap junction morphology. *J. Cell Biol.* 83(2, Pt. 2):269*a* (Abstr.).
2. Andrée, G. 1958. Uber die Natur des Transkapsularen Potentials der Linse. *Arch. Ges. Physiol.* 267:109–116.
3. Baldwin, K. M. 1977. The fine structure of healing over in mammalian cardiac muscle. *J. Mol. Cell Cardiol.* 9:959–966.
4. Baldwin, K. M. 1979. Cardiac gap junction configuration after an uncoupling treatment as a function of time. *J. Cell Biol.* 82:66–75.
5. Bendetti, E. L., I. Dunia, C. J. Bentzel, A. J. M. Vermorken, M. Kibbelaar, and H. Bloemendal. 1976. A portrait of plasmamembrane specializations in eye lens epithelium and fibers. *Biochim. Biophys. Acta.* 457:353–384.
6. Bernardini, G., C. Peracchia, and R. A. Venosa. 1980. Uncoupling of lens fibers. *J. Cell Biol.* In press.
7. Dahl, G., and G. Isenberg. 1980. Decoupling of heart muscle cells: correlation with increased cytoplasmic calcium and with changes of nexus ultrastructure. *J. Membr. Biol.* 53:63–75.
8. DeMello, W. C. 1977. Intercellular Communication. W. C. DeMello, editor. Plenum Press, New York. 87–125.
9. Duncan, G., and A. R. Bushell. 1976. The bovine lens as an ion-exchanger: a comparison with ion levels in human cataractous lenses. *Exp. Eye Res.* 23:341–353.
10. Goodenough, D. A. 1979. Lens gap junctions: a structural hypothesis for nonregulated low-resistance intercellular pathways. *Invest. Ophthalmol. Vis. Sci.* 18:1104–1122.
11. Hama, K., and K. Saito. 1977. Gap junctions between the supporting cells in some austicovestibular receptors. *J. Neurocytol.* 6:1–12.
12. Hanna, R. B., D. C. Spray, P. G. Model, A. L. Harris, and M. V. L. Bennett. 1978. Ultrastructure and physiology of gap junctions of an amphibian embryo, effects of CO_2. *Biol. Bull.* 155:422(Abstr.).
13. Heuser, J. E., T. S. Reese, and D. M. D. Landis. 1975. Preservation of synaptic structure by rapid freezing. *Cold Spring Harbor Symp. Quant. Biol.* 40:17–24.
14. Iwatsuki, N., and O. H. Petersen. 1979. Pancreatic acinar cells: the effect of carbon dioxide, ammonium chloride and acetylcholine on intercellular communication. *J. Physiol. (Lond.).* 291:317–326.
15. Loewenstein, W. R. 1975. Permeable junctions. *Cold Spring Harbor Symp. Quant. Biol.* 40:49–63.
16. Meda, P., A. Perrelet, and L. Orci. 1980. Gap junctions and β-cell function. *Horm. Metab. Res. Suppl.* In press.
17. Meech, R. W., and R. C. Thomas. 1977. The effect of calcium injections on the intracellular sodium and pH of snail neurones. *J. Physiol. (Lond.).* 265:867–879.
18. Peracchia, C. 1973. Low resistance junctions in crayfish. I. Two arrays of globules in junctional membranes. *J. Cell Biol.* 57:54–65.
19. Peracchia, C. 1973. Low resistance junctions in crayfish. II. Structural details and further evidence for intercellular channels by freeze-fracture and negative staining. *J. Cell Biol.* 57:66–76.
20. Peracchia, C. 1974. A structure-function correlation in gap junctions of crayfish. Abstracts of 8th International Congress on Electron Microscopy. J. V. Sanders and D. J. Goodchild, editors. The Australian Academy of Sciences, Canberra A.C.T., Australia. 2:226–227.
21. Peracchia, C. 1977. Gap junctions: structural changes after uncoupling procedures. *J. Cell Biol.* 72:628–641.
22. Peracchia, C. 1977. Changes in gap junctions with uncoupling are a calcium effect. *J. Cell Biol.* 75(2, Pt. 2):65*a* (Abstr.).
23. Peracchia, C. 1978. Calcium effects on gap junction structure and cell coupling. *Nature (Lond.).* 271:669–671.
24. Peracchia, C. 1980. Structural correlates of gap junction permeation. *Int. Rev. Cytol.* 66: 81–146.
25. Peracchia, C., G. Bernardini, and L. L. Peracchia. 1979. Uncoupling mechanism: a hypothesis. *J. Cell Biol.* 83(2, Pt. 2):86*a* (Abstr.).
26. Peracchia, C., and A. F. Dulhunty. 1974. Gap junctions: structural changes associated with changes in permeability. *J. Cell Biol.* 63(2, Pt. 2):263*a* (Abstr.).
27. Peracchia, C., and A. F. Dulhunty. 1976. Low resistance junctions in crayfish: structural changes with functional uncoupling. *J. Cell Biol.* 70:419–439.
28. Peracchia, C., and L. L. Peracchia. 1978. Orthogonal and rhombic arrays in gap junctions exposed to low pH. *J. Cell Biol.* 79(2, Pt. 2):271*a* (Abstr.).
29. Peracchia, C., and L. L. Peracchia. 1980. Gap junction dynamics: reversible effects of divalent cations. *J. Cell Biol.* 87:708–718.
30. Raviola, E., D. A. Goodenough, and G. Raviola. 1978. The native structure of gap junctions rapidly frozen at 4°K. *J. Cell Biol.* 79(2, Pt. 2):229*a* (Abstr.).
31. Riley, M. V. 1970. Ion transport in damaged lenses and by isolated lenses epithelium. *Exp. Eye Res.* 9:28–37.
32. Rose, B., and R. Rick. 1978. Intracellular pH, intracellular free Ca^{++}, and junctional cell-cell coupling. *J. Membr. Biol.* 44:377–415.
33. Turin, L., and A. Warner. 1977. Carbon dioxide reversibly abolishes ionic communication between cells of early amphibian embryo. *Nature (Lond.).* 270:56–57.
34. Turin, L., and A. E. Warner. 1980. Intracellular pH in early *Xenopus* embryos: its effect on current flow between blastomeres. *J. Physiol. (Lond.).* 300:489–504.
35. Unwin, P. N. T., and G. Zampighi. 1980. Structure of the junctions between communicating cells. *Nature (Lond.).* 283:545–549.
36. Weingart, R., and W. Reber. 1979. Influence of internal pH on r_i of Purkinje fibers from mammalian heart. *Experientia.* 35:17(Abstr.).